

Magneto-Optical Trapping of Holmium Atoms

J. Miao, J. Hostetter, G. Stratis, and M. Saffman

*Department of Physics, University of Wisconsin,
1150 University Avenue, Madison, Wisconsin 53706*

(Dated: December 3, 2024)

We demonstrate sub-Doppler laser cooling and magneto-optical trapping of the rare earth element Holmium. Atoms are loaded from an atomic beam source and captured in six-beam $\sigma_+ - \sigma_-$ molasses using a strong $J = 15/2 \leftrightarrow J = 17/2$ cycling transition at $\lambda = 410.5$ nm. Due to the small difference in hyperfine splittings and Landé g -factors in the lower and upper levels of the cooling transition the MOT is self-repumped without additional repump light, and deep sub-Doppler cooling is achieved with the magnetic trap turned on. We measure the leakage out of the cycling transition to metastable states and find a branching ratio $\sim 10^{-5}$ which is adequate for state resolved measurements on hyperfine encoded qubits.

The magneto-optical trap (MOT) is a standard and very widely used tool in cold atom physics. To date MOT operation has been demonstrated for about 30 different neutral elements. Operation of a MOT on an open transition which allows for pumping into metastable states which are not cooled requires “repump” light to return atomic population to the levels participating in laser cooling. The rare earth lanthanides did not originally appear amenable to laser cooling due to the presence of an open f shell (except for Yb which was laser cooled in 1999[1]), and a correspondingly complex atomic structure. It was recognized by McClelland that the lanthanides are amenable to laser cooling due to the presence of cycling transitions between odd(even) parity ground states with angular momentum J and even(odd) parity excited states with angular momentum $J' = J + 1$. MOT operation was first demonstrated with an open f shell lanthanide in 2006 using Er[2]. That demonstration was followed in 2010 by demonstration of MOTs for Dy[3] and Tm[4]. In this work we report on the operation of a Ho MOT loaded from an atomic beam with and without laser slowing[5]. The Doyle group has also recently demonstrated lanthanide MOTs including Ho using buffer gas precooling of an atomic beam [6].

Interest in laser cooling and trapping of lanthanide atoms is motivated by several topics in current research. Quantum degenerate bosonic and fermionic gases of Dy[7, 8], and Er[9, 10] open up new research directions due to the large magnetic moments Er ($6 \mu_B$), Dy ($10 \mu_B$) which provide for much stronger dipolar interactions than are present in the more widely studied alkali gases. Ho has one stable isotope ^{165}Ho , which is bosonic with nuclear spin of $I = 7/2$ and a ground electronic configuration $[\text{Xe}]4f^{11}6s^2$. The ground state term is $^4I^\circ$, $J = \frac{15}{2}$ giving eight hyperfine levels $F_g = 4 \dots 11$. There are large magnetic interactions since the magnetic moment of $9\mu_B$ is only 10% smaller than Dy. Ho is distinguished by having 128 hyperfine-Zeeman states, the largest number of any stable atomic isotope. This large number of states is of interest for collective encoding of multi-qubit quantum registers[11, 12]. Implementation of collective encoding will rely on Rydberg blockade interactions[13] in a dense atomic sample. The demonstration of sub-Doppler laser

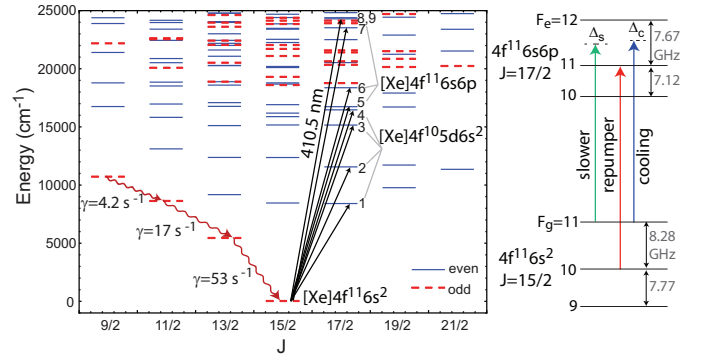


FIG. 1. (color online) Energy levels of Ho. The upper levels of the cycling and cooling transitions are labeled 1-7. The diagram on the right shows the cooling, repumper, and slowing light used on the 410.5 nm transition to level $|e\rangle$.

TABLE I. Ho cycling and cooling transitions. The columns list the vacuum wavelength, natural linewidth, and Doppler cooling limit ($T_D = \hbar\gamma/2k_B$).

Transition	$\lambda(\text{nm})$	$\gamma/2\pi(\text{MHz})$	Doppler limit(μK)
1	1193.	unknown	–
2	867.3	unknown	–
3	660.9	unknown	–
4	608.3	0.038 ^a	0.95
5	598.5	0.146 ^{b,c}	3.5
6	545.3	unknown	–
7	425.6	1.59 ^{b,c}	76.
8	412.1	2.3 ^{b,c}	110.
9	410.5	32.5 ^{b,c}	780.

Energies are taken from [14].

^a Linewidth derived from oscillator strength value reported in [15], ^b Ref. [16], ^c Ref. [17].

cooling, MOT operation, and optical cycling transitions with fractional leakage rates at the 10^{-5} level reported here are first steps towards Rydberg spectroscopy and qubit encoding in Ho atoms.

The level diagram of Ho together with cycling transitions suitable for cooling is shown in Fig. 1. The ground

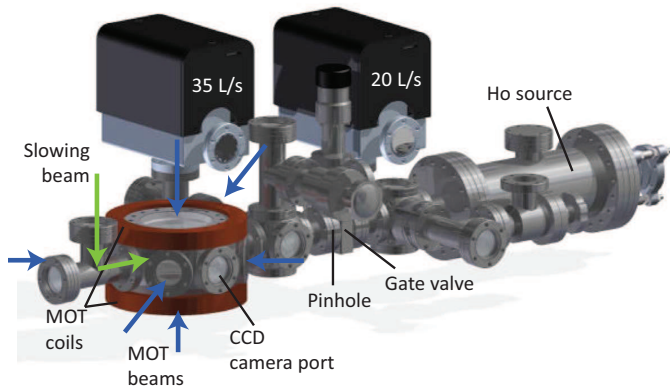


FIG. 2. Vacuum and laser cooling setup. The length of the apparatus from end to end is about 1 m.

state has $J = 15/2$ with odd parity. There are nine dipole allowed transitions to levels with even parity and $J = 17/2$. Since there are no odd parity levels with $15/2 \leq J \leq 19/2$ in between the ground state and the upper levels of the six transitions labeled 1-6 these transitions are cycling. Relevant transition parameters are given in Table I. The 410.5 nm transition from the ground state to $[\text{Xe}]4f^{11}6s6p(^1P)$, $J = 17/2$ at 24361 cm^{-1} (labeled 9 in Fig. 1) is not cycling since there are odd parity levels above the ground state accessible by electric dipole decay from $|e\rangle$. Nevertheless a closer examination of the odd parity levels below $|e\rangle$ with $15/2 \leq J \leq 19/2$ reveals that almost all possible transitions have $|\Delta j| > 1$ on a single electron or are forbidden due to intercombination spin changes. The only transition which is allowed for single electron jumps is $|e\rangle - |4f^{11}5d6s(^1D)$, $J = 17/2$ at a transition energy of 475 cm^{-1} . This transition is very weak due to the ω^3 factor in the expression for the radiative linewidth, with ω the transition frequency. We can roughly estimate the decay rate using hydrogenic orbitals which gives $\gamma' \sim 4000. \text{ s}^{-1}$. This is likely to be an upper limit on the decay rate since the quantum defects are unknown and may substantially reduce the radial integral compared to the hydrogenic value. To the extent that LS coupling is a good description for the level structure of Ho we conclude that the cooling transition with $|g\rangle$ as an upper level will have small leakage since $\gamma'/\gamma \sim 10^{-5}$.

The experimental apparatus is shown in Fig. 2. A water cooled effusion cell with Ta crucible operated at $T = 1150 \text{ C}$ provides a beam of Ho atoms with a mean velocity of 510 m/s . The atomic beam passes through a 0.25 cm diameter tube to prevent outflow of melted Ho from the horizontally oriented effusion cell, and a 0.25 cm diameter aperture for differential pumping before entering the MOT chamber. Two ion pumps provide a base pressure of 10^{-9} mbar in the MOT chamber. A pair of electric coils provide a quadrupole magnetic field with a gradient of up to 0.4 T/m (vertical axis) and 0.2 T/m (horizontal axis). The cooling beams were arranged in a standard

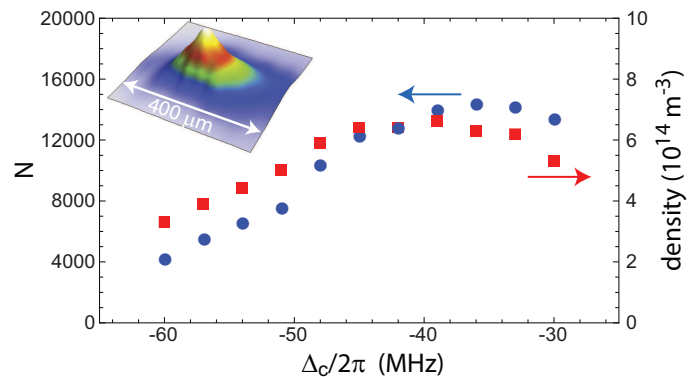


FIG. 3. (color online) Number of trapped atoms (circles) and peak density (squares) as a function of cooling light detuning with the slower light turned on and the repump light turned off. The magnetic field gradient was 0.3 T/m . The inset shows a fluorescence image of the trapped atoms at -36 MHz detuning.

6 beam $\sigma_+ - \sigma_-$ configuration. The beams had Gaussian waists ($1/e^2$ intensity radius) of 2.4 mm and total incident power of 40 mW which was doubled by retro-reflecting the beams. The cooling light was detuned by $\Delta_c \sim -1.5\gamma$ from the $F_g = 11 \rightarrow F_e = 12$ cycling transition. Repump light was tuned to $F_g = 10 \rightarrow F_e = 11$ and overlapped with all MOT beams. In addition a circularly polarized slowing beam counterpropagating to the atomic beam was detuned by $\Delta_s = -2\pi \times 320 \text{ MHz}$ from the $F_g = 11 \rightarrow F_e = 12$ transition. The slowing beam had a power of 140 mW and was focused to a waist of $1. \text{ mm}$. Measurements of the MOT atom number and density were made with an electron multiplying charge coupled device (EMCCD) camera using either fluorescence imaging or absorption imaging with an additional beam tuned to be resonant with the cooling transition. All laser beams were derived from a frequency doubled Ti:Sa laser (M² Solstis with ECD-X) providing up to 1.5 W of 410.5 nm light. The laser was locked to the cooling transition using saturation spectroscopy in a hollow cathode lamp. The frequency and power level of the cooling, repump, and slowing light was controlled by acousto-optic modulators.

The hyperfine energies shown in Fig. 1 were calculated from known values of the A and B constants for the ground state[18] and measured values for the excited state. We measured the hyperfine constants of the upper level of the cooling transition using modulation transfer spectroscopy in the hollow cathode lamp. Fits to our data gave $A = 654.9 \pm 0.3$, $B = -620 \pm 20 \text{ MHz}$. These values agree well with earlier measurements reported in [19].

With the slowing beam turned on, but no repump light, we achieved a typical MOT population of $N \sim 1.5 \times 10^4$ and atomic density of $n_a \sim 6.5 \times 10^{14} \text{ m}^{-3}$ as shown in Fig. 3. The atom number measurement was calibrated by integrating the detected EMCCD MOT image using

the measured camera sensitivity to 410.5 nm light and an integration time of 50 ms. The measurement relies on knowing the rate of scattered photons per atom which we estimated by

$$r = \gamma \rho_{ee} = \frac{\gamma}{2} \frac{I_T/I_s}{1 + 4\Delta_c^2/\gamma^2 + I_T/I_s}. \quad (1)$$

Here ρ_{ee} is the excited state fraction, I_T is the total intensity of the six MOT beams and for the saturation intensity we use $I_s = 2.76 \times I_{sc}$. Here $I_{sc} = 614$ W/m² is the saturation intensity for the cycling transition $|F_g = 11, M = 11\rangle \leftrightarrow |F_e = 12, M = 12\rangle$ and the factor of $2.76 = 3(2 \times 11 + 1)/(2 \times 11 + 3)$ accounts for averaging over Zeeman substates and the random light polarization in the MOT region.

When the repumper was turned on tuned to the $F_g = 10 \rightarrow F_e = 11$ transition the atom number values in Fig. 3 increased by less than 1%. The negligible influence of the repump light is due to the fact that the cooling light also repumps population in $F_g = 10$ much faster than the depumping rate out of $F_g = 11$. The depumping rate due to Raman transitions via $F_e = 10$ or 11 is calculated by averaging over M levels and light polarization, and accounting for the branching ratios of the fluorescence decay. We find

$$r_R = \gamma^3 \left[\frac{I}{36(2I + 1)\Delta_{F_e=F_g}^2} + \frac{5(2I - 1)(2F_g - 1)}{432(2I + 1)(2F_g + 1)\Delta_{F_e=F_g-1}^2} \right] \frac{I_T}{I_{sc}}. \quad (2)$$

In this expression $I = 7/2$ is the nuclear spin, $F_g = 11$ is the F value for the lower level of the cycling transition, $\Delta_{F_e=F_g} = \Delta_{(F+1)_e, F_e} + \Delta_c$, $\Delta_{F_e=F_g-1} = \Delta_{(F+1)_e, (F-1)_e} + \Delta_c$ are the detunings of the MOT light from $F_e = 11$ and $F_e = 10$, and we have assumed the light is far detuned so that we may replace factors of $(1 + 4\Delta^2/\gamma^2 + I_T/I_s)^{-1}$ by $\gamma^2/(4\Delta^2)$. The excited state hyperfine splittings shown in Fig. 1 are $\Delta_{12,11} = 2\pi \times 7.67$ GHz and $\Delta_{12,10} = 2\pi \times 14.79$ GHz. We find that for $\Delta_c = -2\gamma$, the largest detuning we have used, $r_R = 550$ s⁻¹ and $r_R/r = 1.5 \times 10^{-5}$. There is also depumping due to leakage to metastable states. The rate for this process we estimate below to be negligible compared to the Raman rate. The total depumping rate is therefore $< 3 \times 10^3$ s⁻¹. This rate is balanced by the repumping rate for the Raman process $F_g = 10 \rightarrow F_e = 11 \rightarrow F_g = 11$. The cooling light is detuned from the $F_g = 10 \rightarrow F_e = 11$ transition by -610 MHz $+ \Delta_c/2\pi \sim 650$ MHz. The resulting repumping rate is about 2×10^5 s⁻¹.

The ratio of the depumping to repumping rates implies that about 1.5% of the population is in $F_g = 10$ which is consistent with our measurements. Thus, even without a separate repumper the atoms are pumped with close to 99% purity into the $F_g = 11$ level. Further pumping

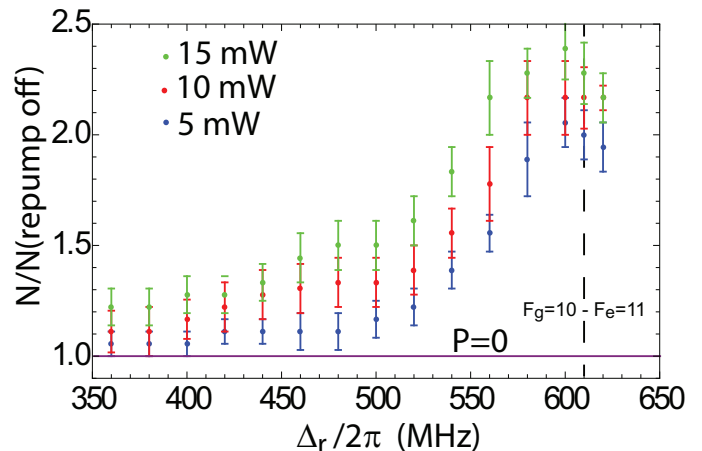


FIG. 4. MOT population as a function of repumper detuning relative to the $F_g = 10 \rightarrow F_e = 11$ transition, and repumper power, with the slowing beam off. The population is normalized to the value with no repumper. The data stops at 620 MHz which was the limit of the AOM used for frequency shifting.

into a specific Zeeman sublevel as a starting point for quantum state control experiments has not been demonstrated, but should be straightforward using an additional π polarized beam tuned to $F_g = 11 \rightarrow F_e = 11$ for pumping into $M = 0$, or a σ_+ polarized beam tuned to $F_g = 11 \rightarrow F_e = 12$ for pumping into $M = 11$.

The effect of the repumper is more significant when the MOT is operated without a slowing beam. In this case the MOT captures only a very small fraction of the low velocity tail of the atomic beam and the loading rate is reduced by almost three orders of magnitude, resulting in a very small MOT with $N = 40$ atoms, again without a repumper. Turning on the repumper increases N by a factor of up to 2.5, depending on the detuning of the repumper, as shown in Fig. 4. The increase in atom number cannot be due to additional repumping since, as explained above, the cooling light acts as its own repumper. We instead interpret the data as being due to the repump light cooling and trapping additional atoms on the $F_g = 10 \rightarrow F_e = 11$ transition. The high temperature atomic source creates a beam which we assume to be uniformly distributed among ground Zeeman states. Since there are 23 Zeeman states in $F_g = 11$ and 21 in $F_g = 10$ we expect roughly a factor of 2 increase, which is in reasonable agreement with the data. No such increase is seen when the slower is on since the slower light is only effective for atoms in $F_g = 11$ and the additional loading of unslowed $F_g = 10$ atoms is negligible.

As shown in Fig. 5 we observe deep sub-Doppler cooling well below $T_D = 780$ μ K using $\sigma_+ - \sigma_-$ MOT beams. Data were acquired by observing MOT expansion and fitting to Gaussian density profiles. The theoretical dependence of the molasses temperature with respect to

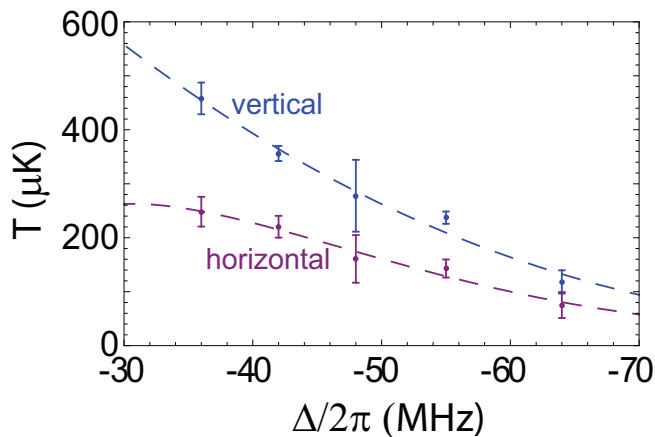


FIG. 5. (Color online) MOT temperature with quadrupole magnetic field on versus detuning at saturation parameter $I/I_s = 1.1$. The Doppler temperature is $780 \mu\text{K}$.

detuning is given by[20]

$$T = T_0 + \frac{\hbar\gamma^2}{2k_B|\Delta|} \frac{I}{I_s} \left(a + \frac{b}{1 + 4\Delta^2/\gamma^2} \right) \quad (3)$$

with a, b constants and T_0 the low intensity temperature limit. Equation (3) reproduces the observed dependence on detuning quite well. Due to the near equality of the ground state $F_g = 11$ and excited state $F_e = 12$ g -factors, 0.82 and 0.83, temperatures reaching ten times below the Doppler limit are achieved with relatively small detunings and with the quadrupole MOT field on during the entire cooling phase.

In order to further study the internal state dynamics we loaded the MOT to steady state with the slowing beam on and then measured the decay lifetime with the slowing beam turned off which greatly reduces the loading into the MOT. Lifetime data was taken with the quadrupole field on giving magnetic trapping and with the 3D molasses light either on or off. The MOT population decay can be modeled with the rate equation[21]

$$\frac{dN}{dt} = R_{\text{off}} - [(1 - \rho_{ee})\Gamma_{\text{bg}} + \rho_{ee}(\Gamma_{\text{la}} + \Gamma_{\text{ms}})]N - \beta N^2$$

where R_{off} is the loading rate with the slowing beam off, Γ_{bg} accounts for losses due to background collisions with ground state atoms, Γ_{la} is the loss rate due to light assisted collisions between optically excited and background atoms[22], Γ_{ms} is the loss rate due to scattering into metastable states, and β accounts for losses from collisions of trapped atoms. Leakage into metastable states may lead to atom loss since the metastable states do not interact with the cooling light and the fraction of atoms which are not magnetically trapped will

drift away. The lowest energy odd parity states with $J = 15/2, 13/2, 11/2, 9/2$ are fine structure levels of the ground term. They decay via magnetic dipole transitions which have been calculated in the LS coupling approximation. The resulting lifetimes indicated in Fig. 1 range from 0.02 to 0.24 s. Also the lowest energy even parity states with $J = 17/2, 19/2, 21/2$ are expected to be long lived, but with lifetimes that are unknown.

With the molasses light off we can set $R_{\text{off}} = \rho_{ee} = 0$ and we observe a rapid decay due to β followed by a slower decay which is fit to give $\Gamma_{\text{bg}} = 0.77 \text{ s}^{-1}$. With the molasses light on at detuning -1.1γ we calculate $\rho_{ee} = 0.2$ and observe an increased exponential decay rate of $\Gamma_{\text{on}} = 1.4 \text{ s}^{-1}$. The exponential loss rate with the molasses light on can be expressed as $\Gamma_{\text{on}} = (1 - \rho_{ee})\Gamma_{\text{bg}} + \rho_{ee}(\Gamma_{\text{la}} + \Gamma_{\text{ms}})$. The scattering rate into metastable states can therefore be estimated from

$$\gamma_{\text{ms}} = \frac{\Gamma_{\text{ms}}}{\rho_{ee}} = \frac{\Gamma_{\text{on}} - (1 - \rho_{ee})\Gamma_{\text{bg}}}{\rho_{ee}^2} - \frac{\Gamma_{\text{la}}}{\rho_{ee}}$$

The light assisted loss rate is not known, or easily calculable. Setting it to zero we derive an upper bound for the scattering rate into metastable states of $\gamma_{\text{ms}} \leq 20. \text{ s}^{-1}$. This value is comparable to those reported for Yb[23] and Tm[4] but is substantially smaller than that found previously for ^{165}Ho [6] ($\gamma_{\text{ms}} = 895 \text{ s}^{-1}$), using a different method. The reason for the discrepancy in these measurements is not known. The branching ratio to metastable states is very small $\gamma_{\text{ms}}/(\gamma + \gamma_{\text{ms}}) \sim 10^{-7}$ so that loss out of the cycling transition is dominated by Raman transitions to other ground hyperfine levels with a branching ratio we estimated above to be $\sim 10^{-5}$. On the basis of these measurements we conclude that it should be possible to make high fidelity hyperfine state resolved measurements of Ho atoms, which will be important for qubit experiments.

In conclusion, we demonstrated a magneto-optical trap of Ho atoms. Single frequency molasses light together with a slowing beam is sufficient to load a MOT with 15000 atoms at temperatures below $100 \mu\text{K}$ from an atomic beam source. The atoms are prepared in the $F_g = 11$ level with probability close to 99% and fractional leakage rates out of the cooling transition are shown to be less than $\sim 10^{-5}$. Future work will explore the use of this cold sample as the starting point for quantum control experiments which take advantage of the large manifold of hyperfine states.

This work was supported by NSF grant PHY0969883 and the University of Wisconsin graduate school. We are grateful to Jake Covey, Johannes Nipper, and Hannes Gorniaczyk for contributions at early stages of this experiment.

[1] K. Honda, Y. Takahashi, T. Kuwamoto, M. Fujimoto, K. Toyoda, K. Ishikawa, and T. Yabuzaki, Phys. Rev. A

- [2] J. J. McClelland and J. L. Hanssen, *Phys. Rev. Lett.* **96**, 143005 (2006).
- [3] M. Lu, S. H. Youn, and B. L. Lev, *Phys. Rev. Lett.* **104**, 063001 (2010).
- [4] D. Sukachev, A. Sokolov, K. Chebakov, A. Akimov, S. Kanorsky, N. Kolachevsky, and V. Sorokin, *Phys. Rev. A* **82**, 011405(R) (2010).
- [5] J. Miao, J. Hostetter, G. Stratis, and M. Saffman, *Bull. Am. Phys. Soc.* **58**, U2.00005 (2013).
- [6] B. Hemmerling, G. K. Drayna, E. Chae, A. Ravi, and J. M. Doyle, arXiv:1310.3239 (2013).
- [7] M. Lu, N. Q. Burdick, S. H. Youn, and B. L. Lev, *Phys. Rev. Lett.* **107**, 190401 (2011).
- [8] M. Lu, N. Q. Burdick, and B. L. Lev, *Phys. Rev. Lett.* **108**, 215301 (2012).
- [9] K. Aikawa, A. Frisch, M. Mark, S. Baier, A. Rietzler, R. Grimm, and F. Ferlaino, *Phys. Rev. Lett.* **108**, 210401 (2012).
- [10] K. Aikawa, A. Frisch, M. Mark, S. Baier, R. Grimm, and F. Ferlaino, *Phys. Rev. Lett.* **112**, 010404 (2014).
- [11] E. Brion, K. Mølmer, and M. Saffman, *Phys. Rev. Lett.* **99**, 260501 (2007).
- [12] M. Saffman and K. Mølmer, *Phys. Rev. A* **78**, 012336 (2008).
- [13] M. Saffman, T. G. Walker, and K. Mølmer, *Rev. Mod. Phys.* **82**, 2313 (2010).
- [14] A. Kramida, Y. Ralchenko, J. Reader, and NIST ASD Team, <http://physics.nist.gov/asd>, version 5.1 (2013).
- [15] V. N. Gorshkov and V. A. Komarovskii, *Opt. Spectrosc.* **47**, 631 (1979), [*Opt. Spectrosc. (USSR)* **47**, 350 (1979)].
- [16] E. A. D. Hartog, L. M. Wiese, and J. E. Lawler, *J. Opt. Soc. Am. B* **16**, 2278 (1999).
- [17] G. Nave, *J. Opt. Soc. Am. B* **20**, 2193 (2003).
- [18] L. S. Goodman, H. Kopfermann, and K. Schlüpmann, *Naturwiss.* **49**, 101 (1962).
- [19] C. I. Hancox, Ph.D. thesis, Harvard (2005).
- [20] J. Dalibard and C. Cohen-Tannoudji, *J. Opt. Soc. Am. B* **6**, 2023 (1989).
- [21] D. Sesko, T. Walker, C. Monroe, A. Gallagher, and C. Wieman, *Phys. Rev. Lett.* **63**, 961 (1989).
- [22] J. E. Bjorkholm, *Phys. Rev. A* **38**, 1599 (1988).
- [23] T. Loftus, J. R. Bochinski, R. Shivitz, and T. W. Mossberg, *Phys. Rev. A* **61**, 051401 (2000).